

# Turbulence Closure Modelling in Coastal Waters

Hans Burchard, Ulf Gräwe, Peter Holtermann, Knut Klingbeil and Lars Umlauf

## Summary

In this paper the use of turbulence closure models in coastal ocean models is reviewed. Two-equation turbulence closure models are argued to be an optimal compromise between efficiency and accuracy for the purpose of calculating diapycnal fluxes of momentum, heat and tracers in coastal ocean modelling. They provide enough degrees of freedom to be calibrated to the most prominent properties of coastal ocean mixing, but are still numerically robust and computationally efficient. Isopycnal mixing schemes are briefly reviewed as well. Major implementational and numerical aspects are presented, with some focus on the inherent problem of numerically-induced mixing which together with the physically-induced mixing gives the effective mixing in ocean models. Vertically adaptive coordinates are presented as one possibility to reduce numerical mixing. Finally, three coastal ocean simulation examples from the General Estuarine Transport Model (GETM) which is coupled to the turbulence module of the General Ocean Turbulence Model (GOTM) are given. These examples include thermocline mixing in the Northern North Sea, physically and numerically induced mixing in the Western Baltic Sea as well as basin-wide mixing in the Central Baltic Sea. All three examples highlight the importance of using well-calibrated turbulence closure models together with vertically adaptive coordinates.

## Keywords

coastal ocean modelling, turbulence closure modelling, numerical mixing, adaptive coordinates, General Ocean Turbulence Model (GOTM), General Estuarine Transport Model (GETM)

## Zusammenfassung

*In diesem Artikel wird die Anwendung von Turbulenzschließungsmodellen in numerischen Modellen für den Küstenozean dargestellt. Zwei-Gleichungs-Turbulenzschließungsmodelle stellen für die Berechnung von diapycnischen Impuls-, Wärme- und Konzentrationsflüssen im Küstenozean einen optimalen Kompromiss zwischen Effizienz und Genauigkeit dar. Diese Modelle gewährleisten ausreichende Freiheitsgrade, um sie für die wichtigsten Eigenschaften der Vermischung im Küstenozean zu kalibrieren, sind aber immer noch numerisch robust und effizient im Bedarf an Rechenzeit. Isopyknische Vermischungsschemata werden ebenfalls kurz dargestellt. Die wichtigsten Aspekte der Implementierung und Numerik werden diskutiert, wobei der Schwerpunkt auf der numerisch induzierten Vermischung liegt, die zusammen mit der physikalisch induzierten Vermischung erst die effektive Vermischung in Ozeanmodellen ergibt. Vertikal-adaptive Koordinaten werden als eine Möglichkeit dargestellt, die numerische Vermischung zu reduzieren. Abschließend werden Beispiele von Simulationen im Küstenozean mit dem General Estuarine Transport Model (GETM) in Kopplung mit dem Turbulenzmodul des General Ocean Turbulence Model (GOTM) gezeigt. Diese Beispiele umfassen Vermischung in der Thermokline der nördlichen*

Nordsee, physikalisch und numerisch induzierte Vermischung in der westlichen Ostsee sowie beckenweite Vermischung in der zentralen Ostsee. Diese drei Beispiele zeigen, wie wichtig die Verwendung von gut kalibrierten Turbulenzschließungsmodellen zusammen mit vertikal-adaptiven Koordinaten in der Modellierung von Prozessen im Küstenozean ist.

## Schlagwörter

Küstenozeanmodellierung, Turbulenzschließungsmodellierung, numerische Vermischung, adaptive Koordinaten, General Ocean Turbulence Model (GOTM), General Estuarine Transport Model (GETM)

## Contents

1	Introduction .....	70
2	Turbulence closure modelling.....	72
2.1	Two-equation closure models as work horses for parameterising vertical turbulent fluxes.....	72
2.2	Parameterisations for horizontal turbulent fluxes .....	75
3	Numerical and implementation aspects .....	76
4	Coastal ocean modelling examples.....	77
4.1	Thermocline mixing in the Central North Sea.....	78
4.2	Physical and numerical mixing in the Western Baltic Sea.....	79
4.3	Basin-wide mixing in the Central Baltic Sea.....	81
5	Conclusions.....	83
6	References .....	84

## 1 Introduction

Turbulent dissipation and mixing is of tremendous importance for the dynamics of the coastal ocean and the associated transports of heat, salt, suspended matter and biogeochemical solutes. Direct observations of mixing and dissipation are hampered by the stochastic character of the turbulence and its strong spatial and temporal variability. Meaningful observations of turbulence can only be carried out at single locations and at relatively large instrumental effort. Typical instrumentation includes free-falling turbulence microstructure profilers, operated from board, as well as high-resolution acoustic Doppler velocity measurements on integrated moored platforms. Successful observations of this type in the coastal zone of the North Sea and the Baltic Sea have, for example, been carried out by BECHERER et al. (2011), UMLAUF et al. (2007) and VAN DER LEE and UMLAUF (2011). These observations are indispensable for process studies in coastal waters but, in view of the extreme spatial and temporal intermittency of turbulence, they are usually insufficient to assess the gross turbulent transport and mixing in entire coastal ocean areas such as the basins in the Baltic Sea, tidal estuaries or the German Bight. For such system-wide studies, realistic three-dimensional numerical models are applied, which parameterise the turbulent processes with statistical methods. The turbulence observa-

tions (which are typically accompanied by observations of currents and stratification) are then invaluable for model calibration and validation.

Major processes for which marine turbulence is essential are for example the annual cycle of mixed layer dynamics (on which the entire primary production depends), sediment transport in highly dynamic waters such as the Wadden Sea or tidal estuaries (on which for example the morphodynamic evolution of these waters depends), processes of estuarine circulation and residual currents in estuaries and tidal inlets (on which residual sediment and solute transports depend), entrainment of ambient waters into buoyant surface plumes (such as river plumes) or dense bottom currents such as the saline inflows into the Baltic Sea, just to name a few.

The three-dimensional shallow water (i.e., hydrostatic) momentum equations for the calculation of the velocity vector ( $u, v, w$ ) are the basis of most coastal ocean models. Examples for such models are the structured-grid models ROMS (Regional Ocean Modelling System, [www.myroms.org](http://www.myroms.org), see e.g. SCHEPETKIN and MCWILLIAMS 2005) and GETM (General Estuarine Transport Model, [www.getm.eu](http://www.getm.eu), see e.g. HOFMEISTER et al. 2010 and references therein) and the unstructured-grid models SELFE ([http://www.stccmop.org/knowledge\\_transfer/software/selfe](http://www.stccmop.org/knowledge_transfer/software/selfe), ZHANG and BAPTISTA 2008) and FVCOM (Unstructured Grid Finite Volume Coastal Ocean Model, <http://fvcom.smast.umassd.edu/FVCOM/>, CHEN et al. 2002). The general form of the momentum equations in these models is as follows (see, e.g., BLUMBERG and MELLOR 1987):

$$\begin{aligned} \partial_t u + \partial_x(uu) + \partial_y(uv) + \partial_z(uw) - \partial_x(2A_h\partial_x u) - \partial_y(A_h(\partial_y u + \partial_x v)) - \partial_z(A_v\partial_z u) = \\ + fv - g\partial_x\eta + \int_z^\eta \partial_x b d\xi \end{aligned} \quad (1)$$

$$\begin{aligned} \partial_t v + \partial_x(vu) + \partial_y(vv) + \partial_z(vw) - \partial_y(2A_h\partial_y v) - \partial_x(A_h(\partial_y u + \partial_x v)) - \partial_z(A_v\partial_z v) = \\ -fu - g\partial_y\eta + \int_z^\eta \partial_y b d\xi \end{aligned} \quad (2)$$

where  $x$  and  $y$  denote the horizontal coordinates,  $z$  the vertical coordinate (positive upward), and  $t$  the time.  $f$  is the Coriolis parameter,  $b = -g(\rho - \rho_0)/\rho_0$  is buoyancy (with gravitational acceleration  $g$ , reference density  $\rho_0$  and potential density  $\rho$ ), and  $\eta$  is surface elevation. Together with equations for temperature and salinity and an equation of state for the calculation of potential density, this system of equations is closed, apart from the determination of the vertical and horizontal eddy viscosities  $A_v$  and  $A_h$ , respectively, and the vertical and horizontal eddy diffusivities,  $K_v$  and  $K_h$ , respectively (the latter are required for the temperature, salinity and other tracer budget equations). For the determination of the vertical eddy viscosity and diffusivities,  $A_v$  and  $K_v$ , turbulence closure modelling is required for which complex and diverse theories are available. The coastal ocean models listed above all use directly coupled (or recoded as in the case of ROMS, see WARNER et al. 2005) versions of the turbulence closure modelling library GOTM (General Ocean Turbulence Model, [www.gotm.net](http://www.gotm.net), UMLAUF and BURCHARD 2005), the underlying theory of which will be presented in Section 2.1. For the modelling of the horizontal eddy viscosity and diffusivity,  $A_h$  and  $K_h$ , typically relatively simple algebraic closures are used, which will briefly be discussed in Section 2.2.

## 2 Turbulence closure modelling

### 2.1 Two-equation closure models as work horses for parameterising vertical turbulent fluxes

Two-equation turbulence closure models have emerged as work horses of coastal ocean modelling during the last decades. The most prominent members of this class of models are the  $k$ - $\varepsilon$  model (RODI 1980; BURCHARD and BAUMERT 1995), the  $k$ - $\omega$  model (WILCOX 1988; UMLAUF et al. 2003), and the  $k$ - $kl$  model (MELLOR and YAMADA 1982), with the turbulent kinetic energy per unit mass (TKE),  $k$ , the dissipation rate of the TKE,  $\varepsilon$ , the turbulent frequency,  $\omega = \varepsilon/k$  and the length scale of the energetic turbulent eddies,  $l$ . Key component of all models of this type is the so-called energy cascading relation,

$$\varepsilon = c_e \frac{k^{3/2}}{l} \quad (3)$$

which connects the energy-containing turbulent motions of scale  $l$  with the dissipation of kinetic energy at the smallest (Kolmogorov) scales ( $c_e$  is a proportionality constant). In analogy to the kinetic theory of ideal gases, the vertical eddy viscosity and eddy diffusivity are determined as proportional to the product of a turbulent length scale (here  $l$ ) and a turbulent velocity scale (here  $k^{1/2}$ ). Using the cascading law in (3), these relations can be re-expressed in their most commonly used forms

$$A_v = c_\mu \frac{k^2}{\varepsilon}, \quad K_v = c'_\mu \frac{k^2}{\varepsilon}, \quad (4)$$

with the non-dimensional stability functions  $c_\mu$  and  $c'_\mu$  which may in general be functions of a number of non-dimensional flow invariants (see below). It could be shown in a series of papers (BURCHARD et al. 1998; BAUMERT and PETERS 2000; UMLAUF et al. 2003; UMLAUF and BURCHARD 2003) that all two-equation models mentioned above are mathematically equivalent in situations where the (advective and turbulent) transport of turbulence quantities is negligible. As these situations determine the basic properties of the turbulence models used in coastal ocean modelling, we limit our following discussion to the most commonly used two-equation turbulence closure model: the  $k$ - $\varepsilon$  model. Within three-dimensional ocean models, the  $k$ - $\varepsilon$  model is generally applied in the following form:

$$\partial_t k + \partial_x (uk) + \partial_y (vk) + \partial_z (wk) - \partial_z \left( \frac{A_v}{\sigma_k} \partial_z k \right) = P + B - \varepsilon \quad (5)$$

$$\partial_t \varepsilon + \partial_x (u\varepsilon) + \partial_y (v\varepsilon) + \partial_z (w\varepsilon) - \partial_z \left( \frac{A_v}{\sigma_\varepsilon} \partial_z \varepsilon \right) = \frac{\varepsilon}{k} (c_1 P + c_3 B - c_2 \varepsilon) \quad (6)$$

with the 5 empirical parameters  $\sigma_k$  and  $\sigma_\varepsilon$  (turbulent Schmidt numbers) and  $c_1$ ,  $c_2$  and  $c_3$ . For the latter parameter, we distinguish between  $c_3^-$  for stable stratification and  $c_3^+$  for unstable stratification.  $P = A_v M^2$  with vertical shear squared  $M^2 = (\partial_z u)^2 + (\partial_z v)^2$  is the shear production (converting mean kinetic energy into TKE), and  $B = -K_v N^2$  with buoyancy frequency squared  $N^2 = \partial_z b$  is the buoyancy production (converting potential

energy to TKE or vice versa). It should be noted that the TKE equation can be directly derived from Reynold-averaging the Navier-Stokes equations, with only one rather straight-forward closure assumption: the down-gradient parameterisation for the turbulent fluxes. The right hand side of the budget equation for the dissipation rate, however, is entirely empirical, assuming dimensional consistency, and a form of the source and sink terms that is analogous to that in the TKE budget.

The five free parameters of the  $k$ - $\varepsilon$  model provide sufficient degrees of freedom to calibrate this model to the most relevant standard flow situations. The basis for calibrating the three parameters on the right hand side of the dissipation rate equation is the assumption of a homogeneous turbulent flow for which all spatial gradients on the left hand side of (5) and (6) vanish, leaving a system of two ordinary differential equations (ODEs). To calibrate  $c_1$ , (3) is used to derive an ODE for the length scale  $l$  from (5) and (6), which has the following form:

$$\partial_t l = c_e \frac{k^{1/2}}{\varepsilon} ((1.5 - c_1)P + (1.5 - c_3)B - (1.5 - c_2)\varepsilon) \quad (7)$$

Using the theoretical argument that shear, which has dimensions of an inverse time, should not determine a length scale (BAUMERT and PETERS 2000),  $c_1 = 1.5$  is required to eliminate the corresponding shear production term on the right hand side of (7). To calibrate  $c_2$ , freely decaying turbulence with  $P = B = 0$  is assumed for which the ODEs for  $k$  and  $\varepsilon$  can be solved for large  $t$  as

$$\frac{k}{k_0} \propto \left( \frac{t}{t_0} \right)^d \quad (8)$$

with the decay rate  $d = -1/(c_2 - 1)$ . Experimentally,  $-1.3 \leq d \leq -1$  has been determined, such that  $1.77 \leq c_2 \leq 2$  is a realistic range for  $c_2$  (see UMLAUF and BURCHARD 2003, for details).

A strategy for calibrating  $c_3^-$  is to consider steady-state solutions for the ODEs for  $k$  and  $\varepsilon$  to eliminate  $P$ . Defining the mixing efficiency as  $\Gamma = -B/\varepsilon$ , the following relation for calculating  $c_3^-$  is obtained:

$$\Gamma = \frac{c_2 - c_1}{c_1 - c_3^-} \quad (9)$$

Since for a stationary, stably stratified shear flow a mixing efficiency of  $\Gamma \approx 0.2$  is a well-established result (OSBORN 1980),  $c_3^-$  can be considered as the calibration parameter for the mixing efficiency (BURCHARD and HETLAND 2010). It should be pointed out that the correct calibration of the model parameter  $c_3^-$  is essential for the performance of the model in stably stratified flows (e.g., in entrainment situations). Note that earlier approaches suggested using the steady-state Richardson number (which has been shown to be in the order of  $\frac{1}{4}$ ) for the calibration of  $c_3^-$  (BURCHARD and BAUMERT 1995). For unstable stratification (convective turbulence with  $B > 0$ ), HOLT and UMLAUF (2008) argued that for the length scale equation in (7) the second term on the right hand side must not be positive, since otherwise there would only be source terms for the length scale equation. This would result into a situation where the source terms could only be balanced by the turbulent transport term (which however would be zero or of the wrong

sign in parts of the water column). Therefore, HOLT and UMLAUF (2008) suggest  $c_3^+ = 1.5$ .

The Schmidt number for the dissipation rate,  $\sigma_\varepsilon$ , is calibrated by the requirement that the dissipation rate equation is consistent with law-of-the-wall scaling for steady-state solutions with  $B = 0$ , where the resulting relation is

$$\sigma_\varepsilon = \frac{\kappa^2}{(c_\mu^0)^{1/2} (c_2 - c_1)} \quad (10)$$

with the von Karman constant  $\kappa = 0.4$  and the equilibrium (for  $P = \varepsilon$ ) value of the viscosity stability function,  $c_\mu^0$  (with a typical value of  $c_\mu^0 = 0.09$ ). Note that the bottom boundary conditions for the TKE and its dissipation rate are usually directly derived from the law of the wall (see BURCHARD and PETERSEN 1999 who could show that flux conditions are numerically more accurate than Dirichlet conditions). Surface boundary conditions are constructed in the same way, using the surface friction velocity as velocity scale. For situations where injection of TKE due to surface wave breaking is relevant, a downward TKE flux and a modified flux of the dissipation rate are applied (UMLAUF and BURCHARD 2003, 2005). Finally, the Schmidt number for the TKE equation,  $\sigma_k$ , can be used to calibrate the experimentally determined spatial decay rate of TKE for grid stirring experiments (UMLAUF and BURCHARD 2003), and should have a value of about unity. With these relations, a consistent parameter set would for example be:

$$c_1 = 1.5; \quad c_2 = 1.9; \quad c_3^- = -0.5; \quad c_3^+ = 1.5; \quad \sigma_k = 1.0; \quad \sigma_\varepsilon = 1.33. \quad (11)$$

The standard  $k$ - $\varepsilon$  model as it is described above is closed by a choice for the turbulent Prandtl number  $P_r^t = A_v / K_v$  which is of the order of unity and may depend on stratification (BURCHARD and BAUMERT 1995). Two-equation models of higher complexity are obtained from so-called algebraic closures of the transport equations for the second moments (e.g., the Reynolds stresses and the turbulent heat fluxes). These models have been shown to result in significant improvements over the standard model, in particular in stratified situations, as discussed in detail e.g. in BURCHARD (2002) and UMLAUF and BURCHARD (2005). Successful algebraic second-moment closures have been provided by CANUTO et al. (2001) and adapted to two-equation models by BURCHARD and BOLDING (2001). In short, the result of these algebraic second moment closures is that the stability functions defined in (4) turn out as functions of the shear number  $M^2\tau^2$  and the buoyancy number  $N^2\tau^2$ , with the turbulent time scale  $\tau = k/\varepsilon$ .

The way how the two-equation models are constructed, they are boundary layer models which would fail in the ocean interior where the interaction between turbulence and internal waves dominates mixing. Therefore, in the interior, where turbulence quantities predicted from solutions of the transport equations for  $k$  and  $\varepsilon$  tend to vanish, a lower threshold for  $k$  and  $\varepsilon$  is implemented. To this end, in stratified flow, the turbulent length scale  $l$  is limited by the Ozmidov scale  $l_O = (\varepsilon/N^3)^{1/2}$ , which can be reformulated as  $\varepsilon > (c_e/c_{\lim})kN$  with  $c_{\lim} = 0.53$  as suggested by GALPERIN et al. (1988). In stably stratified turbulence, the TKE is assumed to be kept on certain levels due to the energy flux from the internal wave field to turbulence, where generally no information about this energy transfer is available in ocean models. Therefore, the TKE is simply limited by a minimum TKE level:  $k \geq k_{\min}$ , where  $k_{\min}$  basically is a calibration parameter for the

eddy viscosity in the stably stratified low energy flow. BURCHARD et al. (2002) could show that observed thermocline eddy viscosities in the Northern North Sea could be reproduced by using a value of  $k_{\min} = 10^{-6}$  J/kg.

## 2.2 Parameterisations for horizontal turbulent fluxes

Whereas in ocean models a consistent theoretical framework for the vertical turbulent fluxes exists, such a rigorous closure for the horizontal fluxes is still missing. Two common approaches used in the coastal ocean modelling community are to either neglect horizontal diffusion (e.g., due to the excess of artificial numerical mixing, see BURCHARD and RENNAU 2008 and Section 3) or to set  $A_h$  to a constant value. The proper choice of  $A_h$  is determined by sensitivity studies. The major criticism against using a constant horizontal viscosity (diffusivity) is that this approach is not scale-sensitive. An increase in grid resolution should lead to a decrease in horizontal viscosity. In the limit of doing Direct Numerical Simulations (DNS) the value of  $A_h$  should vanish (the so far neglected molecular viscosity must be reconsidered in this case). A second drawback of using a constant  $A_h$  is that the spatial structure of the flow is not taken into account. For instance in regions with high horizontal shear or strain the horizontal turbulent fluxes should be higher than in regions of calm waters. Therefore a scale- and flow-sensitive sub-grid closure is needed.

A possible solution is the use of Large Eddy Simulations (LES). Here the energy containing eddies are resolved. However, for most oceanographic applications the numerical effort required for this technique is prohibitively large.

To close the gap, SMAGORINSKY (1963) proposed an LES-type closure for geophysical applications. He proposed a scaling for the horizontal eddy viscosity for a numerical model whose grid-scale lies in the forward energy cascade range of 3D turbulence as proposed by KOLMOGOROV (1941):

$$A_h = c(\Delta x \Delta y) \sqrt{(\partial_x u)^2 + \frac{1}{2} (\partial_y u + \partial_x v)^2 + (\partial_y v)^2} \quad (12)$$

with  $c$  being a constant in the order of  $O(0.1)$ , and  $\Delta x$ ,  $\Delta y$  being the horizontal grid size. As required, this parameterisation is scale-sensitive but also takes the shear and strain of the flow field into account. The only free parameter  $c$  needs to be determined by sensitivity experiments. For instance, HOLT and JAMES (2006) could show that for their application a value of  $c = 0.1$  gave a too rich eddy field (as compared to satellite observations). A value of  $c = 0.4$  resulted in a too smooth velocity field. They concluded that a value of  $c = 0.2$  gave best results.

Smagorinsky's viscosity was a leap forward in understanding the interaction of numerical resolution and physics, and has proven useful in engineering and coastal scale flows. Nevertheless in the last decade the validity of Smagorinsky's underlying assumptions were questioned (e.g., FOX-KEMPER et al. 2008).

The scaling in (12) was derived basing on the assumption that the spectral energy scales as  $E(k) \propto k^{-5/3}$ , with  $k$  being the wavenumber. Moreover, Kolmogorov envisioned a forward energy cascade from large scales to smaller scales. The same holds for the enstrophy. To resolve the Kolmogorov energy cascade in the ocean a resolution in the order of  $O(1\text{cm})$  is necessary, which is far from being feasible today. Additionally,

CHARNEY (1971) showed that at geophysical scales, the turbulence is 2D (geostrophic turbulence) and not isotropic any more. He could show that the energy now scales as  $E(k) \propto k^{-3}$ . Since in most oceanographic applications the Rossby number (the ratio of vorticity and Coriolis frequency) is smaller than one, large parts of the flow are in geostrophic balance and thus described by geostrophic turbulence. Additionally, Charney could show that the enstrophy still shows a forward energy cascade. In contrast to Kolmogorov's 3D turbulence, 2D turbulence shows an inverse cascade of energy. Thus, energy is transferred from smaller scales to the larger scales. To take this fact into account, LEITH (1996) suggested an alternative scaling of the viscosity based on the vorticity.

During a numerical experiment, MENEMENLIS et al. (2006) compared the SMAGORINSKY (1963) and the LEITH (1996) parameterisations of the horizontal viscosity. They concluded that the viscosity scaling should be based on an enstrophy cascade that is reproduced by the LEITH (1996) scaling rather than the SMAGORINSKY (1963) scaling resulting from an inertial energy cascade. However, the LEITH (1996) scaling needs to be adapted such that divergent motions present in 3D simulations do not become unstable or too large such that the vertical advection Courant condition is violated.

The above discussed horizontal viscosities are expected to be less sensitive to subgrid-scale parameterisations than in coarse-resolution modelling exercises. Moreover, they outperform the still applied constant viscosities. However, even high-resolution ocean models are sensitive to subgrid-scale parameterisations, so parameterisation improvement is important. Of course, the range of scales in the ocean is vast and diverse. Phenomena that are substantially smaller than the grid-scale, for instance submesoscale eddies, the loss of geostrophic balance or even microstructure turbulence – will continue to require purely theoretical parameterisations in ocean models for the next few decades at least (e.g., FOX-KEMPER et al. 2008).

### 3 Numerical and implementation aspects

To obtain a modular coupling between a turbulence closure model and a three-dimensional hydrodynamic ocean model, well defined lists of parameters have to be exchanged between the two models. The 3D model needs to receive the eddy viscosity and the eddy diffusivity from the turbulence closure model. Furthermore, since typically turbulence closure models are formulated as one-dimensional water column models, the 3D model has to store the turbulent properties  $k$  and  $\varepsilon$ . In turn, the 1D turbulence closure model has to receive shear  $M$  and stratification  $N$  to calculate the production terms and the surface and bottom friction velocities (as well as the surface and bottom roughness lengths) to calculate the surface and bottom boundary conditions. These properties need to be exchanged at each time step. Since 3D models mostly are based on horizontally and vertically staggered grids, spatial interpolations are needed to locate the exchanged terms in the correct and numerically stable position. This is also essential for Finite Element Models (see, e.g., KÄRNÄ et al. 2012). Since the turbulent time scale is mostly much shorter than the time scales of the hydrodynamics, it is tempting to neglect the 3D advection of  $k$  and  $\varepsilon$ , which has to be managed by the 3D hydrodynamic model. The quality requirements to the applied advection schemes are high, since the turbulent quantities may vary over orders of magnitude on short distances and the resulting values must still be positive. Therefore, relatively expensive positive-definite advection schemes need to

be applied. Although 3D model results neglecting advection of turbulent quantities may often be sufficiently accurate, numerical instabilities may occur due to this neglect. Therefore, in complex realistic flow situations, turbulence advection should be included.

One other essential numerical aspect of turbulence closure modelling is the discretization of the dissipation terms for  $k$  and  $\varepsilon$  to ensure their positivity (which is mathematically guaranteed). The method which is generally used, is the source term linearisation (PATANKAR 1980), see the detailed discussion by BURCHARD et al. (2005).

Finally, it should be noted that the effective dissipation and mixing in ocean modelling generally is higher than the physically calculated mixing based on the turbulence closure. Dissipation and mixing are defined as the decay of variance of velocity or tracers, respectively. As an example the temperature mixing is locally calculated as

$$\chi_\theta = 2K_v(\partial_z\theta)^2 + 2K_h(\partial_x\theta)^2 + 2K_b(\partial_y\theta)^2 \quad (13)$$

with the potential temperature  $\theta$ . It is, however, known that numerical advection of tracers (such as temperature, salinity, suspended matter) generally leads to artificial numerical mixing, which may be of the same order of magnitude as the physical mixing. Methods to exactly quantifying numerical mixing have been developed by BURCHARD and RENNAU (2008) and KLINGBEIL et al. (2014). The latter authors have shown how to extend the numerical mixing analysis to a numerical dissipation analysis. In summary, to assess effective mixing and dissipation in numerical models, the numerical variance decay must be quantified as well. Numerical dissipation and mixing can be reduced by choosing accurate advection schemes, high resolution or adaptive coordinates (HOFMEISTER et al. 2010).

#### 4 Coastal ocean modelling examples

In this section, results from coastal ocean example simulations are shown which demonstrate the essential role of turbulence closure modelling for such regions. All simulations are carried out with the General Estuarine Transport Model (GETM, see e.g. HOFMEISTER et al. 2011), which is coupled to the turbulence closure module of the General Ocean Turbulence Model (GOTM, see UMLAUF and BURCHARD 2005). Details of the turbulence closures included are presented in detail in Section 2.1. For all simulations, bottom and surface following vertically adaptive coordinates (HOFMEISTER et al. 2011) were used to provide high vertical resolutions in (temporally and spatially variable) regions of strong shear or stratification. In the horizontal, spherical coordinates with a staggered C-grid were used. Surface forcing was provided from the German Weather Service local model, while lateral boundary conditions were prescribed from a 1nm GETM simulation for the entire North Sea and Baltic Sea region. Fig. 1 shows the complete model domain for this simulation, of which results along a transect in the North Sea (green line) are discussed in Section 4.1. This North Sea transect demonstrates the relevance of accurate thermocline resolution and diapycnal mixing rates for realistic North Sea modelling. Results for a nested Western Baltic Sea (WBS) simulation with a resolution of about 600 m with focus on numerical mixing are shown in Section 2.2. Finally, results from a 600 m resolution nested simulation of the Central Baltic Sea (CBS) to study effective basin-wide mixing are presented in Section 4.3. The model domains for the WBS and the CBS models are shown in Fig. 1 as well.

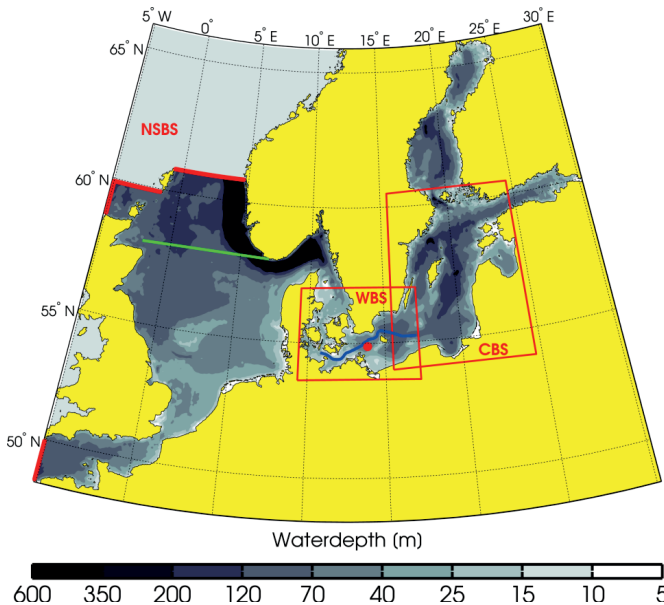


Figure 1: Map auf the North Sea / Baltic Sea 1nm model setup (NSBS). The two red boxes indicate the boundaries of the nested Western Baltic Sea model (WBS) and the Central Baltic Sea (CBS). Additionally, the green line marks the location of the temperature transect in Fig. 2. The blue line indicates the transect as shown in Fig. 4. The red dot shows the position of the MARNET Arkona buoy the data of which is used here for model validation (see Fig. 3).

#### 4.1 Thermocline mixing in the Central North Sea

The Central North Sea is temperature-stratified during summer and well-mixed during winter. Summer stratification starts in spring when turbulent mixing due to tides and wind is sufficiently suppressed by the stratifying effect of the downward surface heat fluxes. Mixing also plays a pivotal role in the primary production of the North Sea. Once in late spring surface nutrients are depleted, nutrient supply to the euphotic zone is limited to upward diapycnal nutrient fluxes from the nutrient-rich bottom waters across the thermocline. The intensity of these fluxes depends largely on the values of eddy diffusivity  $K_v$  in the strongly stratified thermocline region. As discussed in Section 2.1, the eddy viscosity and the eddy diffusivity in this region are controlled by the value for the minimum TKE level,  $k_{min}$ . Fig. 2 shows observed and simulated summer temperature stratification along a 58°N transect across the North Sea. The agreement between the observations (which are limited to a depth range between 10 m and 70 m) and model results is good. Even details of the temperature structure such as a decrease in near-surface temperature and stratification from east to west and the sharpness of the temperature jump in the thermocline region are well-reproduced. The latter is only possible due to the strong accumulation of coordinate layers in the thermocline region which allows for a vertical resolution of locally below 0.2 m (Fig. 2c). The eddy viscosity in the sharp thermocline region is generally above values of  $10^{-6} \text{m}^2 \text{s}^{-1}$ . Apart from the high vertical resolution, the use of vertically adaptive coordinates is strongly reducing artificial numeri-

cal mixing (see also Section 4.2), which would in models with geopotential coordinates dominate the diapycnal mixing and the associated fluxes of nutrients.

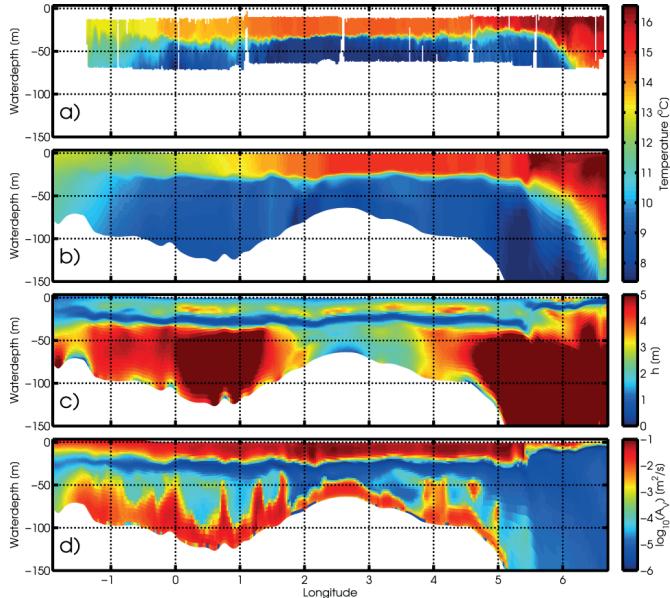


Figure 2: Simulations and model results along a 58°N transect across the North Sea (see the green line in Fig. 1 for the location) on September 03, 2009. a: temperature observed by an undulating CTD profiler (courtesy Bundesamt für Seeschifffahrt und Hydrographie); b: simulated temperature; c: local thickness of adaptive coordinates; d: eddy viscosity.

## 4.2 Physical and numerical mixing in the Western Baltic Sea

Numerical modelling of the Baltic Sea is a challenging task. Simulations of the Baltic Sea must reproduce the water mass exchange through the narrow and shallow Danish Straits, the irregular overflows over the Darss Sill and the Drogden Sill, the emerging bottom gravity currents into the chain of basins in the Baltic proper, the interleaving of inflows at the correct density level, and low mixing levels during stagnation periods in the deep basins. These different demands require a well-designed ocean circulation model with a well-calibrated turbulence closure (Section 2.1). In several studies, it was shown that the General Estuarine Transport Model (GETM) equipped with the General Ocean Turbulence Model (GOTM) provides an excellent numerical model suite to tackle these demands (BURCHARD et al. 2009; HOFMEISTER et al. 2011). For example, HOFMEISTER et al. (2011) presented a validated model for the whole Baltic Sea with a resolution of 1 nm. In order to study local and submesoscale processes, models with higher resolution can be nested into such coarse-grid models. In this section results from a 600 m model of the Western Baltic Sea are presented (see Fig. 1 for the model domain). At the open boundaries in the Kattegat and east of the Bornholm Basin the free surface elevation, depth-integrated velocities and profiles of temperature and salinity are prescribed from the coarse-resolution NSBS model. The simulation was performed with 40 adaptive layers, providing high vertical resolution in boundary layers but also at the evolving

thermo- and haloclines. With these settings the dynamics in the Western Baltic Sea were accurately simulated. Fig. 3 shows a validation against mooring data in the Arkona basin (see Fig. 1 for the location of this autonomous buoy). However, as argued in Section 3, the simulated effective mixing and dissipation is not only a result of the parameterised subgrid-scale effects (physical contribution), but also of the truncation errors of the discrete advection terms (numerical contribution), see Klingbeil et al. 2014. In Fig. 4 the ratios of numerical to physical salt mixing and kinetic energy dissipation are shown along the transect depicted in Fig. 1. In large areas the numerically induced mixing had the same order of magnitude as the physical one. In contrast, the numerically induced dissipation of kinetic energy was at least one order of magnitude smaller than the physical dissipation. These results emphasise the need of accurate advection schemes with reduced numerical mixing and the relevance of well-calibrated turbulence parameterisations for the (physical) dissipation of kinetic energy.

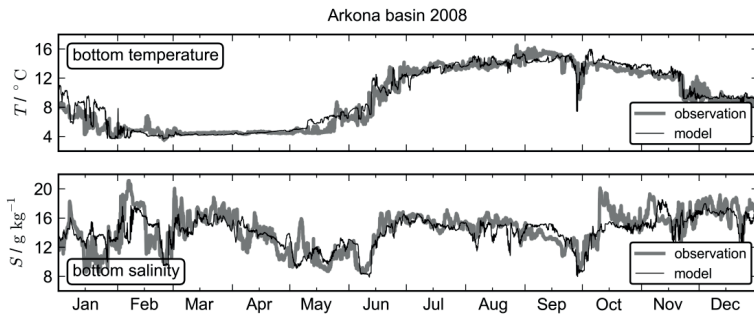


Figure 3: Comparison of time series for observed and simulated bottom temperature and bottom salinity in the Arkona Basin for the year 2008. The observations are from near-bottom (48 m depth) CTD sensor of the MARNET Arkona buoy located in the central Arkona basin (see Fig. 1 for the location).

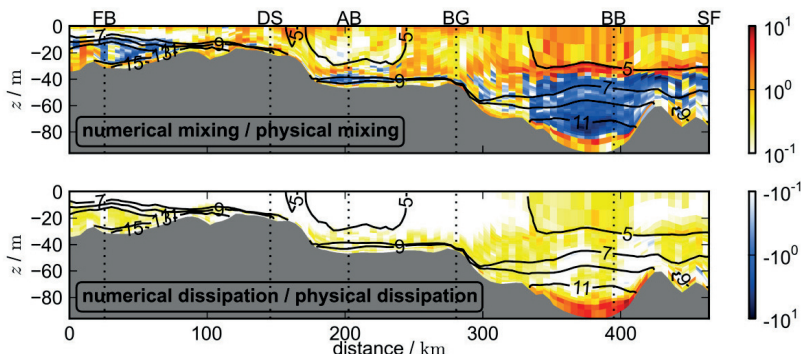


Figure 4: Ratios of numerical to physical salt mixing and kinetic energy dissipation along the transect shown in Fig. 1. Isopycnals are depicted by contour lines. The data are averaged over the period 19-28 Sep 2008. Vertical lines indicate the positions of Fehmarn Belt (FB), Darss Sill (DS), Arkona Basin (AB), Bornholmsgat (BG), Bornholm Basin (BB) and Slupsk Furrow (SF).

### 4.3 Basin-wide mixing in the Central Baltic Sea

The Central Baltic Sea is, similar to the Baltic Sea in general, defined by a chain of basins which are interconnected through sills. The dominant basin is the Gotland Basin which is one of the deepest (up to 240 m depth) and, in terms of the water volume, largest basin of the Baltic Sea.

In contrast to the North Sea, tides are virtually absent in the Central Baltic Sea (FEISTEL et al. 2008), leaving wind forcing as the major energy source for mixing. While the upper water column is directly influenced by wind and atmospheric temperature changes, stratification suppresses turbulence and mixing in the deeper parts of the water column; even during winter, surface mixing extends only down to the halocline, located in approx. 80 m depth. The halocline is defined by the transition of the fresher upper layer waters with salinities of about 8 g/kg to the deeper areas with salinities of up to 13 g/kg. The heating of the surface waters during spring and summer creates a second density interface, the thermocline. The thermocline strongly inhibits the mixing between the colder winter water above the halocline and below the thermocline due to direct atmospheric forcing.

Mixing below the halocline and thermocline, respectively, differs thus, in terms of the processes driving the mixing, from near-surface mixing. The effects of a wind event such as a storm, start, from the perspective of deep water mixing, with the excitation of different types of deep-water motions (e.g., internal and topographic waves). These motions loose their energy by bottom and interior friction, and, to a smaller amount, by mixing (i.e., conversion of kinetic into background potential energy). Different from surface layer mixing, deep-water mixing is therefore only indirectly linked to the wind forcing via the chain of processes described above. AXELL (1998) could show that the deep water mixing in the Gotland Basin increased during the stormier winter season, and HOLTERMANN and UMLAUF (2012) correlated single storm events to increased mixing rates. Numerous deep-water processes are known, see for example Fig. 2 by REISSMANN et al. (2009) for a good overview of the mixing processes in the Baltic Sea. Less well-known is the importance of the different processes to deep-water mixing.

An experiment to study the major mixing processes and mixing rates in the deeper parts of the Central Baltic Sea has been conducted in 2007 by releasing a passive tracer in 200 m depth in the Central Gotland Basin (approx. at C1 in Fig. 5). This experiment was called the Baltic Sea Tracer Release Experiment (BaTRE). The use of the inert tracer gas  $\text{CF}_3\text{SF}_5$ , detectable at very low concentrations, allowed following the tracer patch over a time span of two years. In combination with the tracer release, several moorings had been deployed in the Gotland Basin, and turbulence microstructure measurements had been conducted during the same time (UMLAUF et al. 2008; HOLTERMANN et al. 2012; HOLTERMANN and UMLAUF 2012). One of the key results of the experiment were the substantially different vertical turbulent diffusivities felt by the tracer patch during the initial and later phases of the experiment, respectively. These differences were attributed to the effect of boundary mixing processes that started acting on the tracer cloud after the first boundary contact such that the vertical spread of the tracer increased dramatically. This result was found to be in agreement with direct measurements of the turbulent dissipation rate using a free falling shear-microstructure profiler.

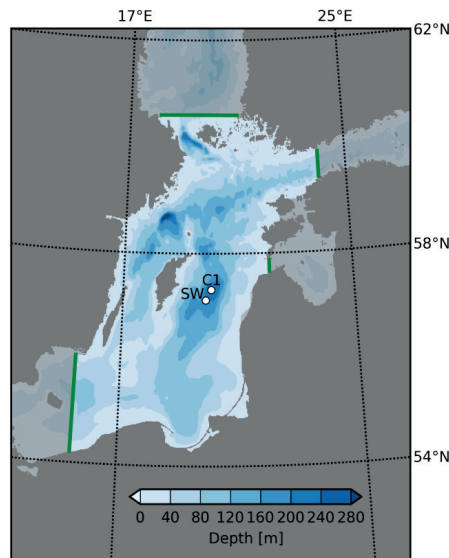


Figure 5: Model domain of the Central Baltic Sea GETM model. Green lines depict the open boundaries. White dots represent the locations of two moorings deployed in the Gotland Basin.

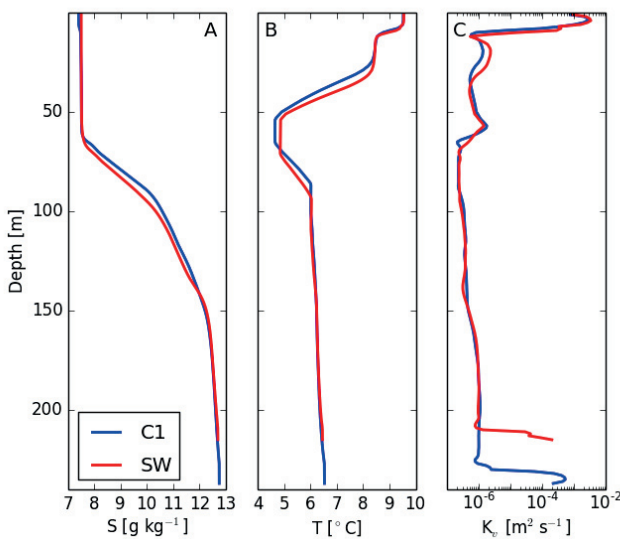


Figure 6: Salinity (A), temperature (B) and turbulent diffusivity (C) at C1 (blue) and SW (red), see as well Fig. 5 for the location of the stations. Data is taken from the GETM model of the Central Baltic Sea at midnight of June 1, 2008.

The consequence of this result, in terms of numerical modelling, is that in the best case, the model should be able to reproduce these different mixing regimes. Good results in that respect have been achieved by a setup for the Central Baltic Sea using the GETM model with 200 vertically adaptive layers and a horizontal resolution of 600 m, see HOLTERMANN et al. (2014). This resolution is rather high in comparison to commonly used models of the Baltic Sea which typically have horizontal grid sizes of 1 nm to 2 nm or coarser (see, e.g., FENNEL et al. 2010). The model was able to reproduce the differences between the low mixing in the interior of the water column and the increased mixing at the basin boundaries and thus the evolution of the tracer cloud.

Fig. 6 shows model results for salinity, temperature and turbulent diffusivity at the stations C1 and SW for a typical summer situation. Clearly visible is the heated upper water column above a layer with colder winter water sandwiched between the thermocline and halocline. Turbulent diffusivities in the upper layers range between  $1 \cdot 10^{-6} \text{m}^2\text{s}^{-1}$  and  $5 \cdot 10^{-3} \text{m}^2\text{s}^{-1}$ . Below the winter water, turbulent diffusivities rarely exceed  $10^{-6} \text{m}^2\text{s}^{-1}$ , illustrating the mechanical insulation of deeper layers from direct atmospheric forcing. Directly above the bottom, however, the turbulent diffusivities increase again as a result of bottom friction. As it can be nicely seen by comparing the eddy diffusivity profiles of the SW and C1 stations in Fig. 6c, the increased bottom boundary turbulent diffusivities occur at different depths. This lateral inhomogeneity between the low  $K_v$  at C1 and the increased  $K_v$  at SW in 210 m is a major reason for the different spreading rates of the passive tracer before and after touching the basin's boundary. Using model results that have been carefully validated against a wealth of observations from the BaTRE experiment, it could be shown that the atmospheric forcing triggered a spectrum of internal waves and sub-inertial motions, which in turn were found to be the main drivers of boundary layer mixing. By successfully reproducing the tracer experiment, the results demonstrated as well the complex interaction between the water masses mixed at the boundaries and the interior water column.

## 5 Conclusions

This study demonstrates the necessity of using sufficiently realistic turbulence closure models as well as sufficiently accurate numerical schemes in models of the coastal ocean. Two-equation turbulence closure models have been demonstrated to provide an optimal solution to this task. Simpler parametric turbulence closure models such as the KPP model (LARGE et al. 1994) as they are often used in large scale ocean models would properly reproduce dynamics such as stratification and de-stratification in proper accuracy. More complex models are typically only applied in idealised situations and have been reported for realistic 3D models of the coastal ocean. For most coastal ocean applications, the physically correct reproduction of the mixing efficiency is key to the predictability for the state of the coastal ocean. In the model applications shown in the present paper, this included suppression of mixing in the seasonal thermocline, entrainment in dense bottom currents and basin-wide mixing. Other coastal ocean processes critically connected to mixing efficiency are for example estuarine circulation, sediment-flow interactions for high sediment concentrations and entrainment of ambient waters into river plumes. The required numerical resolution is here mainly obtained by vertically adaptive coordinates which allow high resolution in regions of high shear and stratification, a pro-

cedure which is of course only effective together with sufficiently accurate advection schemes. Other (non-adaptive) ways of obtaining a high vertical resolution would be simply using a high number of vertical layers (which may often not be affordable) or the use of geopotential coordinates with lateral variation in resolution (BACKHAUS 2008) which however has not yet been tested with coupling to turbulence closure models. One may also use unstructured adaptive Finite Elements in the vertical (PIGGOTT et al. 2008), a method which is still in its infancy in ocean modelling.

Acknowledgements: The German part of the Baltic Monitoring Programme (COMBINE) and the operation of the measuring stations of the German Marine Monitoring Network (MARNET) in the Baltic Sea are conducted by the Baltic Sea Research Institute Warnemünde (IOW) on behalf of the Bundesamt für Seeschifffahrt und Hydrographie (BSH), financed by the Bundesministerium für Verkehr, Bau und Stadtentwicklung (BMVBS). The authors are grateful for the persistent support by Karsten Bolding (Asperup, Denmark) in the development and maintenance of GETM.

## 6 References

- AXELL, L.B.: On the variability of Baltic Sea deep water mixing, *J. Geophys. Res.*, 103(C10), 21,667-21,682, doi:10.1029/98JC01714, 1998.
- BACKHAUS, J.O.: Improved representation of topographic effects by a vertical adaptive grid in vector-ocean-model (VOM). Part I: Generation of adaptive grids, *Ocean Modelling*, 22, 114-127, 2008.
- BAUMERT, H. and PETERS, H.: Second-moment closures and length scales for weakly stratified turbulent shear flows, *J. Geophys. Res.*, 105, 6453-6468, 2000.
- BECHERER, J.; BURCHARD, H.; FLÖSER, G.; MOHRHOLZ, V. and UMLAUF, L.: Evidence of tidal straining in well-mixed channel flow from micro-structure observations, *Geophys. Res. Lett.*, 38, L17611, doi: 10.1029/2011GL049005, 2011.
- BLUMBERG, A.F. and MELLOR, G.L.: A description of a coastal ocean circulation model. In: Heaps, N.S. (Ed.), *Three Dimensional Ocean Models*. American Geophysical Union, Washington, D.C., pp. 1-16, 1987.
- BURCHARD, H.: Applied turbulence modelling in marine waters, vol. 100 of *Lecture Notes in Earth Sciences*, Springer, Berlin, Heidelberg, New York, 229 pp., 2002.
- BURCHARD, H. and BAUMERT, H.: On the performance of a mixed layer model based on the k-e turbulence closure, *J. Geophys. Res.*, 100, 8523-8540, 1995.
- BURCHARD, H. and BOLDING, K.: Comparative analysis of four second-moment turbulence closure models for the oceanic mixed layer. *J. Phys. Oceanogr.*, 31, 1943-1968, 2001.
- BURCHARD, H.; BOLDING, K.; RIPPETH, T.P.; STIPS, A.; SIMPSON, J.H. and SÜNDERMANN, J.: Microstructure of turbulence in the northern North Sea: a comparative study of observations and model simulations, *J. Sea. Res.*, 47, 223-238, 2002.
- BURCHARD, H.; DELEERSNIJDER, E. and STOYAN, G.: Some numerical aspects of turbulence-closure models, pp. 197-206. In: BAUMERT, H.Z.; SIMPSON, J.H. and SÜNDERMANN, J. (eds.), *Marine Turbulence: Theories, Observations and Models*, Cambridge University Press, Cambridge, 630 pp., 2005.

- BURCHARD, H. and HETLAND, R.D.: Quantifying the contributions of tidal straining and gravitational circulation to residual circulation in periodically stratified tidal estuaries, *J. Phys. Oceanogr.*, 40, 1243-1262, 2010.
- BURCHARD, H.; JANSSEN, F.; BOLDING, K.; UMLAUF, L. and RENNAU, H.: Model simulations of dense bottom currents in the Western Baltic Sea. *Cont. Shelf Res.*, 29, 205-220. 2009.
- BURCHARD, H. and PETERSEN, O.: Models of turbulence in the marine environment – a comparative study of two-equation turbulence models, *J. Mar. Syst.*, 21, 29-53, 1999.
- BURCHARD, H.; PETERSEN, O. and RIPPETH, T.P.: Comparing the performance of the k- $\epsilon$  and the Mellor-Yamada two-equation turbulence models, *J. Geophys. Res.*, 103, 10543-10554, 1998.
- BURCHARD, H. and RENNAU, H.: Comparative quantification of physically and numerically induced mixing in ocean models, *Ocean Modelling*, 20, 293-311, 2008.
- CANUTO, V.M.; HOWARD, A.; CHENG, Y. and DUBOVIKOV, M.S.: Ocean turbulence. Part I: one-point closure model. Momentum and heat vertical diffusivities. *J. Phys. Oceanogr.*, 31, 1413-1426, 2001.
- CHARNEY, J.G.: Geostrophic Turbulence, *J. Atmos. Sci.*, 28, 1087-1095, 1971.
- CHEN, C.; LIU, H. and BEARDSLEY, R.C.: An unstructured, finite-volume, three-dimensional, primitive equation ocean model: application to coastal ocean and estuaries. *J. Atmos. Ocean. Tech.*, 20, 159-186, 2002.
- FEISTEL, R.; NAUSCH, G. and WASMUND, N. (Eds.): State and Evolution of the Baltic Sea, 1952-2005. A detailed 50-year survey of meteorology and climate, physics, chemistry, biology, and marine environment, 703 pp., Wiley-Interscience, Hoboken, NJ, USA, 2008.
- FENNEL, W.; RADTKE, H.; SCHMIDT, M. and NEUMANN, T.: Transient upwelling in the central Baltic Sea, *Cont. Shelf Res.*, 30(19), 2015-2026, doi:10.1016/j.csr.2010.10.002, 2010.
- FOX-KEMPER, B.; FERRARI, R. and HALLBERG, R.: Parameterization of mixed layer eddies. Part I: Theory and diagnosis, *J. Phys. Oceanogr.*, 38, 1145-1165, 2008.
- GALPERIN, B.; KANTHA, L.H.; HASSID, S. and ROSATI, A.: A quasi-equilibrium turbulent energy model for geophysical flows. *J. Atmos. Sci.*, 45, 55-62, 1988.
- HOFMEISTER, R.; BECKERS, J.-M. and BURCHARD, H.: Realistic modelling of the exceptional inflows into the central Baltic Sea in 2003 using terrain-following coordinates. *Ocean Modelling*, 39, 233-247, 2011.
- HOFMEISTER, R.; BURCHARD, H. and BECKERS, J.-M.: Non-uniform adaptive vertical grids for 3D numerical ocean models, *Ocean Modelling*, 33, 70-86, 2010.
- HOLT, J.T. and JAMES, I.D.: An assessment of the fine-scale eddies in a high-resolution model of the shelf seas west of Great Britain, *Ocean Modelling*, 13, 271-291, 2006.
- HOLT, J. and UMLAUF, L.: Modelling the tidal mixing fronts and seasonal stratification of the Northwest European Continental shelf, *Cont. Shelf Res.*, 28, 887-903, 2008.
- HOLTERMANN, P.; UMLAUF, L.; TANHUA, T.; SCHMALE, O.; REHDER, G. and WANIEK, J.: The Baltic Sea Tracer Release Experiment. Part 1: Mixing rates, *J. Geophys. Res.*, 117, C01,021, doi:10.1029/2011JC007439, 2012.

- HOLTERMANN, P. and UMLAUF, L.: The Baltic Sea Tracer Release Experiment. Part 2: Mixing processes, *J. Geophys. Res.*, 117, C01,022, doi:10.1029/2011JC007445, 2012.
- HOLTERMANN, P.; BURCHARD, H.; GRÄWE, U.; KLINGBEIL, K. and UMLAUF, L.: Deep-water dynamics and boundary mixing in a non-tidal stratified basin. A modeling study of the Baltic Sea, *J. Geophys. Res. Oceans*, 119, doi:10.1002/2013JC009483, 2014.
- KÄRNÄ, T.; LEGAT, V.; DELEERSNIJDER, E. and BURCHARD, H.: Coupling of a discontinuous Galerkin finite element marine model with a finite difference turbulence closure model, *Ocean Modelling*, 47, 55-64, 2012.
- KLINGBEIL, K.; MOHAMMADI-ARAGH, M.; GRÄWE, U. and BURCHARD, H.: Quantification of spurious dissipation and mixing – Discrete Variance Decay in a Finite-Volume framework, *Ocean Modelling*, doi:10.1016/j.ocemod.2014.06.001, 2014.
- KOLMOGOROV, A.N.: The local structure of turbulence in incompressible viscous fluid for very large Reynolds numbers, *Dokl. Akad. Nauk SSSR*, 30, 301-305, 1941. Reprinted in: *Proc. R. Soc. Lond. A*, 434, 9-13, 1991.
- LARGE, W.G.; MCWILLIAMS, J.C. and DONEY, S.C.: Oceanic vertical mixing: a review and a model with nonlocal boundary layer parameterisation, *Rev. Geophys.*, 32, 363-403, 1994.
- LEITH, C.E.: Stochastic models of chaotic systems, *Physica D*, 98, 481-491, 1996.
- MELLOR, G.L. and YAMADA, T.: Development of a turbulence closure model for geophysical fluid problems. *Rev. Geophys. Space Phys.* 20, 851-875, 1982.
- MENEMENLIS, D.; HILL, C.; ADCROCFT, A.; CAMPIN, J.-M.; CHENG, B.; CIOTTI, B.; FUKUMORI, I.; HEIMBACH, P.; HENZE, C.; KÖHL, A.; LEE, T.; STAMMER, D.; TAFT, J. and ZHANG, J.: NASA supercomputer improves prospects for ocean climate research, *Am. Geophys. Union*, 86(9), 95-96, 2005.
- OSBORN, T.R.: Estimates of the local rate of vertical diffusion from dissipation measurements. *J. Phys. Oceanogr.*, 10, 83-89, 1980.
- PATANKAR, S.V.: Numerical Heat Transfer and Fluid flow. McGraw-Hill, New York, 1980.
- PIGGOTT, M.D.; GORMAN, G.J.; PAIN, C.C.; ALLISON, P.A.; CANDY, A.S.; MARTIN, B.T. and WELL, M.R.: A new computational framework for multi-scale ocean modelling-based on adapting unstructured meshes, *Int. J. Numer. Meth. Fluids*, 56, 1003-1015, 2008.
- REISSMANN, J.; BURCHARD, H.; FEISTEL, R.; HAGEN, E.; LASS, H.U.; MOHRHOLZ, V.; NAUSCH, G.; UMLAUF, L. and WIECZOREK, G.: State-of-the-art review on vertical mixing in the Baltic Sea and consequences for eutrophication, *Progr. Oceanogr.*, 82, 47-80, 2009.
- RODI, W.: Turbulence models and their applications in hydraulics, *Tech. Rep., Int. Assoc. for Hydraul. res.*, Delft, The Netherlands, 1980.
- SHCHEPETKIN, A.F. and MCWILLIAMS, J.C.: The Regional Ocean Modeling System: A split-explicit, free-surface, topography following coordinates ocean model, *Ocean Modelling*, 9, 347-404, 2005.
- SMAGORINSKY, J.: General circulation experiments with the primitive equations, *Month. Weather Rev.*, 91, 99-164, 1963.

- UMLAUF, L.; ARNEBORG, L.; BURCHARD, H.; FIEKAS, V.; LASS, H.U.; MOHRHOLZ, V. and PRANDKE, H.: The transverse structure of turbulence in a rotating gravity current, *Geophys. Res. Lett.*, 34, L08601, doi:10.1029/2007GL029521, 2007.
- UMLAUF, L. and BURCHARD, H.: A generic length-scale equation for geophysical turbulence models, *J. Mar. Res.*, 61, 235-265, 2003.
- UMLAUF, L. and BURCHARD, H.: Second-order turbulence closure models for geophysical boundary layers. A review of recent work, *Cont. Shelf Res.*, 25, 795-827, 2005.
- UMLAUF, L.; BURCHARD, H. and HUTTER, K.: Extending the k-omega turbulence model towards oceanic applications, *Ocean Modelling*, 5, 195-218, 2003.
- UMLAUF, L.; TANHUA, T.; WANIEK, J.J.; SCHMALE, O.; HOLTERMANN, P. and REHDER, G.: Hunting a new tracer, *EOS, Transactions American Geophysical Union*, 89(43), 419-419, 2008.
- VAN DER LEE, E.M. and UMLAUF, L.: Internal-wave mixing in the Baltic Sea: Near-inertial waves in the absence of tides. *J. Geophys. Res.*, 116, C10016, doi:10.1029/2011JC007072, 2011.
- WARNER, J.C.; SHERWOOD, C.R.; ARANGO, H.G. and SIGNELL, R.P.: Performance of four turbulence closure models implemented using a generic length scale method, *Ocean Modelling*, 8, 81-113, 2005.
- WILCOX, D.C.: Reassessment of the scale-determining equation for advanced turbulence models. *AIAA Journal*, 26, 1299-1310, 1988.
- ZHANG, Y. and BAPTISTA, A.M.: SELFE: A semi-implicit Eulerian-Lagrangian finite-element model for cross-scale ocean circulation. *Ocean Modelling*, 21, 71-96, 2008.